ELSEVIER Nuclear Instruments and Methods in Physics Research B 132 (1997) 87–92

NIM B
Beam Interactions with Materials & Atoms

# Functional behaviour of solar bleached thermoluminescence in calcites

I. Liritzis *, Y. Bakopoulos

*Academy of Athens, Research Center for Astronomy and Applied Mathematics, 14 Anagnostopoulou str., Athens 106 73, Greece*

Received 21 February 1997; revised form received 13 May 1997

**Abstract**

In thermoluminescence (TL) measurements and solar bleaching experiments of limestones, the residual TL signal due to sunlight exposure is expressed by a combination of one or two exponential components with some constant term, but in some cases a stretched exponential fit is plausible. The behaviour in such residual TL curves may correspond to a fractal electron traps-centers distribution in the crystal. © 1997 Elsevier Science B.V.

*Keywords:* Thermoluminescence; Calcites; Bleaching; Fractal; Exponential

## 1. Introduction

The thermoluminescence (TL) phenomenon includes the thermal activation of charge carriers (electrons and holes) and their radiative recombination. All these transitions occur among levels within the energy gap of the dielectric crystal under consideration [1,2].

The bleaching of TL of minerals (quartz, feldspar) by sunlight has been used as the basic principle for TL dating of sediments (deep-sea, loess, fluvial, and lacustrine sediments) [3–5]. The same principle has been employed for the dating of archaeological carved megalithic limestone buildings [6].

Pieces of limestone rocks derived from 12 Greek archaeological monuments have been studied. Their colours ranged from pale white to reddish. The solar bleaching of TL has been reported elsewhere [7]. Here, emphasis will be given to the functional form of residual TL after solar bleaching.

## 2. Instrumentation-measurements

Sample preparation and measurement followed standard procedures [1,7,8]. All aliquots (washed with acetic acid, $\varphi < 40$ μm) were exposed to natural daylight conditions (mainly bright sun but with some spells of occasional overcast, in Bordeaux). Prior to any exposure, three of these aliquots recorded the geological TL by heating to 450°C. Normalisation of either of the two prominent TL peaks at 280 ± 5°C and 350 ± 5°C was performed with a second monitor beta dose. The normalised residual TL, following exposure to

* Corresponding author. Tel.: 01 36 13 589; fax: 01 36 606.


*PII* S0168-583X(97)00380-7

sunlight, was plotted as a function of the exposure time (Figs. 1–4). The dispersion from the mean varied between 2% and 10%, per exposure time, especially during the first 10 hours.

The TL glow-curves [7] varied in shape and intensity, but with a common presence of the 280°C peak.

## 3. Functional behaviour of residual TL decay

All the solar bleached TL curves follow a complex exponential function (Figs. 1–4). Although computer simulations of optical bleaching of TL and optically stimulated luminescence signals have accounted for such functional behaviour in quartz [9], our work on calcites extends the current interest on the luminescence mechanism of optical bleaching in calcites.

In the TL phenomenon, the decay of residual TL after exposure to sunlight as a function of exposure time is described by an exponential de-excitation model. This may be a simple exponential,

$$\mathrm{TL}(t) = C_1 e^{-\lambda t} + C_0, \quad (1)$$

or a double exponential,

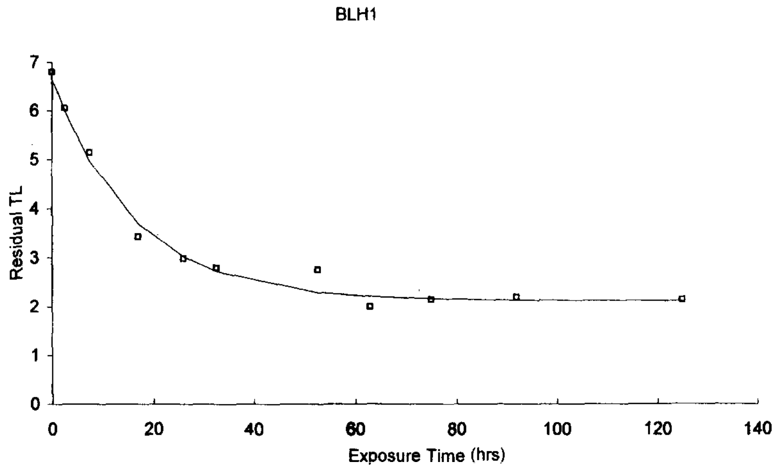


Fig. 1. Sample BLH1. Residual curves of solar bleaching of TL. Experimental data (squares) and theoretical model (line) (see Table 1), for integration temperature region 260–280°C.

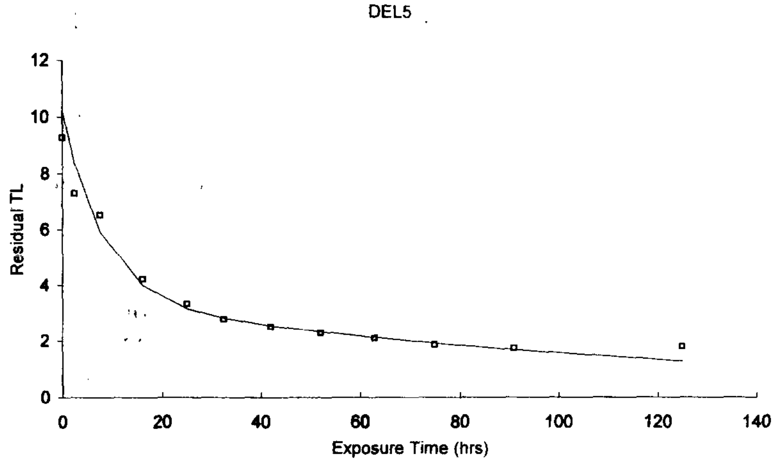


Fig. 2. As in Fig. 1 for DEL5.

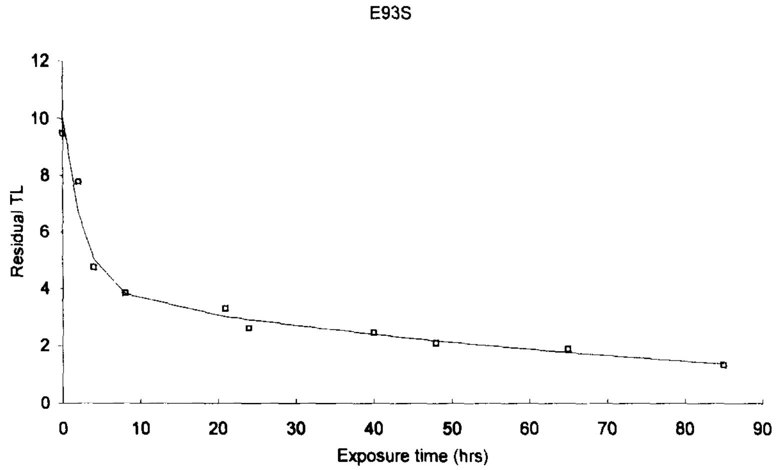


Fig. 3. As in Fig. 1 for ESg3.

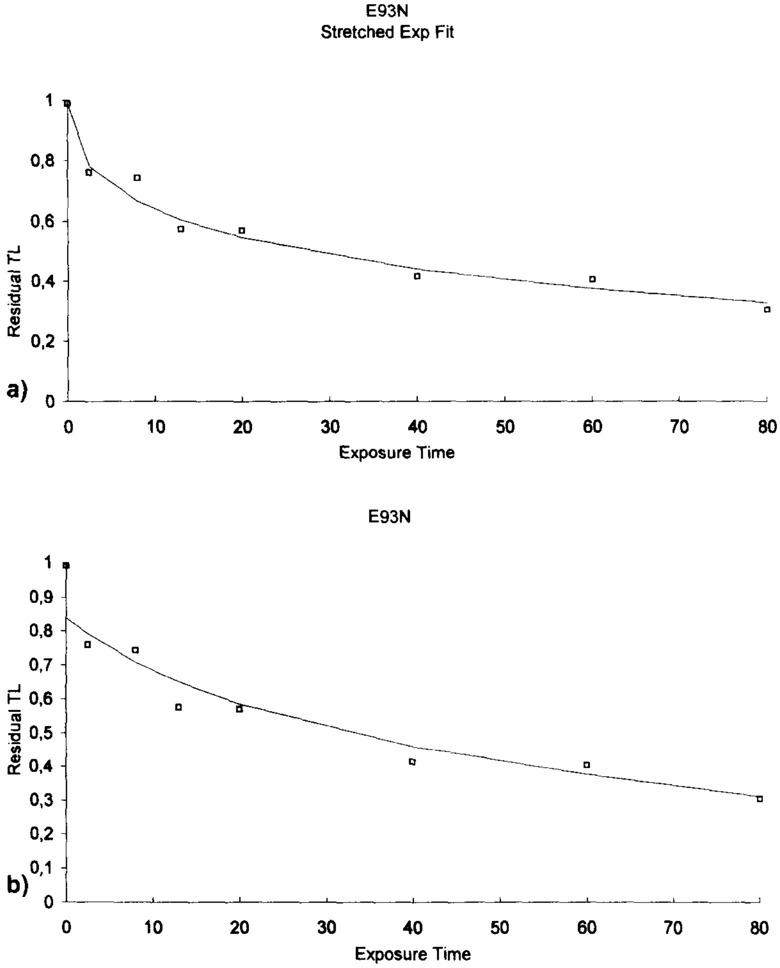


Fig. 4. As in Fig. 1 for Eg3N for 250–300°C, stretched exponential (a), and simple exponential (b) (see Table 1).

$$\mathrm{TL}(t) = C_1 e^{-\lambda_1 t} + C_2 e^{-\lambda_2 t} + C_0, \quad (2)$$

where $C_0$ is a constant background.

The recombination (or de-excitation) rates for the photon emission (luminescence), $\lambda_1$ and $\lambda_2$, are related to the lattice defects in the crystal. For a discrete trap energy spectrum in the lattice, the TL($t$) curve is the sum of discrete exponential components. However, the function occasionally behaves as a stretched exponential term:

$$\mathrm{TL}(t) = C_1 e^{-(\tilde{\lambda} t)^a}, \quad (3)$$

where $0 < a \leqslant 1$.

Computation of the functional forms followed the following procedure: (1) Each data point consisting of three measurements was averaged and the TL residual data were converted to log-lin scale; (2) examination of the linearity of the log-lin scale; (3) fit one or two linear curves in the log-lin scale, with linear regression, usually the first few points (1–4) and subsequent ones; (4) converting the linear curves of log-lin scale to their respective exponential forms; (5) subtracting the exponential component(s) expressed in linear form, from the original data of the linear scale; (6) taking the logarithm of the residuals, if (here, always) a linear curve was obtained in the log-lin scale, then the respective exponential is computed. Alternatively, from Eq. (3) above, if the data points do not seem to have followed obvious straight lines, then the stretched exponential form was searched for as follows: Take the logarithm of the data in the log-lin scale and normalise all data to the first point (i.e. to one), for $t = 0$. The new model is described below. It should be mentioned that the scatter of data depends upon the weather conditions (sunshine, cloudy, etc.), since the present experimental results refer to solar bleaching of natural conditions, as well as to TL measurement alone. Therefore, the criterion for accepting a straight line or not bears a subjectivity index.

Although the $R$-sq. may indicate the best fit of the log-lin data distribution – a straight line or an exponential-like fit – in several cases where $R$-sq. between the two fittings differs a little, one may accept the stretched exponential alone or with the presence of an exponential type or straight line, for the distribution of point defects.

Table 1 gives the functional forms and associated coefficients. A wide range of variation of the $C$'s coefficients and recombination rates ($\lambda$) is observed. The variation of $\lambda_2$ of $0.019 \pm 0.030$ characterises the experimental evidence of a slow bleaching rate of TL for the latter part of the decay curve, and the non-discernibility between a straight line and an exponential term.

One way to support the above model is to consider the TL($t$) curve as the sum of a continuous spectrum of simple exponentials on the basis of a fractal distribution of point defects in the crystal lattice:

$$\mathrm{TL}(t) = C_1 e^{-(\tilde{\lambda} t)^a} \sim C_1 \int_0^{\infty} P(\lambda) e^{-\lambda t}\, \mathrm{d}\lambda, \quad (4)$$

where $\lambda$ belongs to $[0, +\infty)$, and $\tilde{\lambda}$ is the mean value of recombination (de-excitation) rates $\lambda$, which represent a continuous or fractal distribution of recombination centers in the crystal.

If we assume that the distribution function $P(\lambda)$ corresponds to an analogous point defects distribution function $F(x, y, z)$, then the relation $P(\lambda)\,\mathrm{d}\lambda \sim F(x, y, z)\,\mathrm{d}V$ holds. This means that electron de-excitation rate distribution value is proportional to the point defect distribution value on $\mathrm{d}V$ at a position $(x, y, z)$.

The above relationships indicate a fractal distribution of point defects in the crystal lattice.

## 4. Discussion of the new model

A possible interpretation is that the creation of electron traps in the crystal followed a cascade process, where $1 \to 2 \to 4 \to 8 \to \cdots 2n \to \cdots$ The result of such a process is the creation of an uncountable but totally disconnected set (three dimensional dust) of the point defects (traps and holes or luminescent centers). The result is a fractal set on the crystal of dimension $D'$, where $0 < D' \leqslant 3$.

As an electron travels in the crystal volume along a one-dimensional trajectory path, the interaction between this path and the above mentioned fractal set defines a new fractal set with dimension $D = a$, $0 < D \leqslant 1$. Then, this picture is reflected on

Table 1
Functional forms of simple and stretched exponentials and associated coefficients of the first ($C_1$, $\lambda_1$) and second ($C_2$, $\lambda_2$) exponential terms, for the 285 °C and 350 °C TL peaks, respectively. In $R$-sq. column, the numbers refer to the first and second exponential term, respectively. The numbers in parenthesis, under each sample, refer to the number of fitted data points.

| Sample | $C'_0$ | $C_1$ | $\lambda_1$ | $C_2$ | $\lambda_2$ | $R$-sq |
|---|---|---|---|---|---|---|
| LIG93-1 250–320 (1–3, 3–6) | – | 2.7 | −0.131 | 6.42 | −0.0014 | v.l, 0.45 |
| 330–345 (1–3, 3–6) | | 1.71 | −0.327 | 3.64 | −0.0055 | v.l, 0.99 |
| E93-1 (1–4, 5–11) | – | 6.11 | −0.236 | 3.87 | −0.001 | 0.91, vl[a] |
| BLH4 (2–5, 5–10) | – | 4.84 | −0.056 | 4.67 | −0.008 | vl, 0.95 |
| BLH1 260–280 (1–6) | 2.11 | 4.53 | −0.062 | – | – | 0.96 |
| 320–340 (3–6, 7–10) | | 4.61 | −0.031 | 4.31 | −0.0014 | 0.77, 0.95 |
| DEL1 (1–4, 5–9) | | 4.47 | −0.083 | 5.05 | −0.013 | 0.99, 0.99 |
| stretched exp. | | 0.99 | −0.033 | $a = 0.92 \pm 0.06$ | | 0.92 |
| DEL2 (2–5) | 1.45 | 8.29 | −0.072 | | | 0.98 |
| DEL3 (1–5, 6–12) | 1.60 | 0.96 | −0.017 | 4.68 | −0.061 | 0.81, 0.97 |
| stretched exp. | | 8.1 (not-norm.) | −0.033 | $a = 0.67 \pm 0.05$ | | 0.98 |
| DEL4 (3–6, 8–11) | – | 13.05 | −0.063 | 4.09 | −0.0047 | 0.99, 0.98 |
| stretched exp. | | 20 (not-norm.) | −0.06 | $a = 0.44$ | – | 0.96 |
| DEL5 (1–6, 6–11) | – | 6.65 | −0.127 | 3.56 | −0.0083 | 0.95, 0.98 |
| DEL8Gr (1–5, 6–9) | – | 1.59 | −0.059 | 5.15 | −0.0053 | 0.94, 0.60[b] |
| E93S (1–4, 5–11) | – | 6.2 | −0.39 | 3.92 | −0.0122 | 0.96, 0.94 |
| E93N | | 0.18 | −0.075 | 0.65 | −0.009 | 0.4[b], 0.94 |
| stretched exp. | | 0.99 | −0.02 | $a = 0.44$ | · | 0.93 |
| *Averages*: | 1.7 ± 0.5 | 5 ± 2.9 | −0.122 ± 0.107 | 3.8 ± 1.5 | −0.019 ± 0.03 | |

[a] vl: very low significance, possibly best fit a straight line (constant term).
[b] The low $R$-sq. imply high scatter and possibly presence of a constant term.

the recombination rate of the electrons, which means that $P(\lambda)$ is defined over a set of values of $\lambda$, which in turn is a "one dimensional dust", with fractal dimension $0 < D = a \leqslant 1$. (The graphic representation of such a law of distribution $P(\lambda)$ is known as the "Devil's staircase" [10]).

In practice, it appears as a power law:

$$P(\lambda) = C'_0 \lambda^{-D}. \tag{5}$$

To study the function $\mathrm{TL}(t) = C'_0 \mathrm{e}^{-(\tilde{\lambda} t)^a}$, we write

$$\mathrm{TL}(t)/C'_0 = \varphi(t) = \mathrm{e}^{-(\tilde{\lambda} t)^a}, \tag{6}$$

$$\mathrm{Ln}(\varphi(t)) = -(\tilde{\lambda} t)a, \tag{7}$$

$$\mathrm{Ln}(-\ln(\varphi(t))) = a \ln t + a \ln \tilde{\lambda}. \tag{8}$$

From Eqs. (6) and (8), when

$$t = 1/\tilde{\lambda}, \text{ then } \mathrm{Ln}\, t + \mathrm{Ln}\, \tilde{\lambda} = 0. \tag{9}$$

From Table 1, for stretched exponentials, the value $t = 1/\tilde{\lambda}$ is obtained for $\varphi(t) = 1/\mathrm{e}$. A plausible explanation is the presence in the calcitic lattice of a fractal distribution of traps and centers or point defects.

## 5. Conclusion

It has been shown that the functional behaviour of solar bleached TL decay in calcites (limestones) can be represented by a multi-exponential function. In particular, a stretched exponential model may describe a fractal point defect distribution in the crystal lattice.

## Acknowledgements

We are thankful to the National Greek Committee of UNESCO for funding the present project, a part of which is this paper.

## References

[1] M.J. Aitken, Thermoluminescence dating, Academic Press, London, 1985.
[2] S.W.S. McKeever, Thermoluminescence of solids, Cambridge University Press, Cambridge, 1985.
[3] A.G. Wintle, D.J. Huntley, Can. J. Earth Sci. 17 (3) (1980) 348.
[4] V. Mejdahl, Rad. Prot. Dosim. 17 (1986) 219.
[5] G.W. Berger, Progress in luminescence dating methods for quaternary sediments, in: N.W. Rutter, N.R. Catto (Eds.), Dating Methods for Quaternary Deposits, Geotext 2, Geological Association of Canada, 1995, p. 81.
[6] I. Liritzis, C.R. Acad. Sci. Paris, Ser. II 319 (1994) 603.
[7] I. Liritzis, P. Guibert, F. Foti, M. Schvoerer, Nucl. Instr. and Meth. B 117 (1996) 260.
[8] A.G. Wintle, Modern Geol. 5 (1975) 165.
[9] S.W.S. McKeever, M.F. Morris, Radiat. Meas. 23 (1994) 301.
[10] B. Mandelbrot, The Fractal Geometry of Nature, Freeman, New York, 1983.